Feasibility of Brain Lesion Characterization at 1.5T – Whole-Brain Susceptibility Mapping Using A Homogeneous Lesion Constraint

F. Schweser[1], A. Deistung[1], B. W. Lehr[1], and J. R. Reichenbach[1]

[1]Medical Physics Group, Department of Diagnostic and Interventional Radiology, Jena University Hospital, Jena, Germany

INTRODUCTION – Susceptibility weighted MR phase data provide anatomical contrast complementary to magnitude data [1-3] by directly reflecting local magnetic field changes. Recently, ambitious approaches were presented for the challenging problem of inverting the magnetic field to magnetic susceptibility [4-6]. However, most of the presented studies demonstrated fairly poor fidelity, were *ex vivo* studies, required excessive data acquisition, and/or data were acquired at ultra-high field strength. In this contribution, we present an improved method for high-quality whole-brain susceptibility mapping based on a single standard clinical low-field SWI-dataset. Feasibility of *in vivo* lesion characterization is demonstrated for clinical patient data (n=10). Furthermore, it was shown by numerical simulation that only minimal susceptibility differences with respect to the surrounding tissue may be obtained for cavernous lesions.

MATERIALS AND METHODS – Susceptibility mapping was performed based on a spatial-domain algorithm which was previously presented by our lab [7]. The algorithm has been further improved by implementing a homogeneous-lesion constraint, as proposed by de Rochefort et al. [4]. However, rather than to make the problem over-determined our intention was to resolve the issue of signal voids concomitant with solid lesions. Furthermore, a new type of regularization was used which we call "residual regularization": Instead of $\phi = A\chi$, the highly underdetermined system $\phi = A\chi + \beta\sigma$ was solved for $\chi(\vec{r})$ and $\sigma(\vec{r})$ in a minimum-norm sense, where the amount of regularization is controlled by the scalar value β.

Numerical Model: A numerical model was generated of a spherical lesion (radius 20 voxels) in a homogeneous tissue matrix (512^3 voxel). The field was computed by fast forward-field calculation [8] and was 4x down-sampled using a Fourier-based method (lesion radius 5 voxels).

Data Acquisition and Pre-Processing: Whole-brain data were acquired with a fully flow compensated 3D gradient-echo sequence (TE/TR/FA=40ms/60ms/25°, voxel size=0.5×0.5×2 mm³) on an 1.5T MR-scanner (Magnetom Vision Plus, Siemens Medical Solutions). Phase data were corrected using a 3D phase-unwrapping algorithm [10] and spherical-mean-value estimation (radius/thickness 10/1 voxel) [11]. A mask with unreliable phase values (unwrapping artifacts and low SNR) was generated based on automatic evaluation of magnitude and phase data. Regions of lesions and tumor tissue were manually identified and semi-automatically defined by image intensity using MRIcro software.

Inversion: The simulated field was inverted both using spherical lesion constraints of different radii and without lesion constraints. Only phase values of the tissue matrix were used where the sub-voxel gradient of the field did not exceed a certain threshold and the simulation was repeated for various thresholds. For the patient data the lesions were incorporated as homogeneity-constraints into the inversion. Voxels with unreliable phase values were excluded from the problem. The inversion was repeated with successively eroded lesion constraints (up to 5x) to estimate the impact of lesion size on computed susceptibility. Resulting maps were post-processed by removing noise-speckles and smoothing using MRIcro.

RESULTS – The numerical simulation (results not shown) indicated that it is only possible to determine the product of lesion volume and susceptibility if only the maximum lesion size is known from the signal void. Thus, only the minimum susceptibility difference of a lesion may be obtained with respect to surrounding tissue. Representative views of the *in vivo* field and susceptibility maps of two patients are shown in Fig. 1. Inversion of the field to susceptibility is clearly discernable (green arrows). Patient A suffered from acute lymphocytic leukemia (ALL) [9] and demonstrated multiple cerebral hemorrhages. Patient B demonstrated several para- and diamagnetic lesions and a calcified, highly vascularized brain-tumor. Determined susceptibilities of the lesions of patient B are depicted in Fig. 2 over the lesion size. Clear identification and differentiation of para- and diamagnetic lesions was possible.

DISCUSSION AND CONCLUSIONS – We demonstrated feasibility of high-quality susceptibility mapping based on standard clinical SWI phase data. The presented concept enables semi-automated brain lesion characterization in clinical practice and may in principle be fully automated. Striking artifacts and underestimation of lesion susceptibilities [16] in presence of signal-voids were overcome by spatial domain inversion and homogeneous lesion constraints.
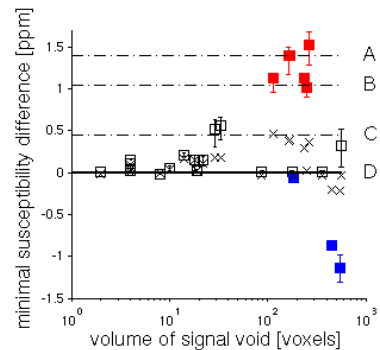

FIG. 2: Minimal susceptibility (SI-units) of the lesions of patient B relative to brain parenchyma over size of the signal void. Lines mark susceptibility of fat (A, [12]), deox. blood (B, [13], Hct 0.42), venous blood (C, OEF 0.426 [14]), and parenchyma/ox. blood (D, [13]). Calcifications are diamagnetic [15]. Potential hemorrhages and calcifications are marked with red and blue, respectively. Squares with error-bars mark minimum and maximum susceptibility for 1…5 erosions. Crosses mark corresponding values calculated without lesion constraints.

REFERENCES – [1] Rauscher A et al. *Am J Neuroradiol,* 26(4):736-42, 2005. [2] Deistung A et al. *Magn Reson Med*, 60(5):1155-68, 2008. [3] Duyn JH et al. *Proc Natl Acad Sci Unit States Am,* 104(28):11796-801, 2007. [4] de Rochefort L et al. *Magn Reson Med*, 60(4):1003-9, 2008. [5] de Rochefort L et al. *Med Phys*, 35(12):5328-39, 2008. [6] Liu T et al. *Magn Reson Med*, 61(1):196-204, 2009. [7] Deistung A et al. *ISMRM*, p2931, 2009. [8] Marques JP and Bowtell R. *Concepts Magn Reson B Magn Reson Eng*, 25(1):65-78, 2005. [9] Kullnig, P et al. *Radiology Case Reports* 2(4), 2007. [10] Abdul-Rahman HS et al. *Appl Optics*, 46(26):6623-35, 2007. [11] Li L. *Magn Reson Med*, 46(5):907-16, 2001. [12] Hopkins JA and Wehrli FW. *Magn Reson Med*, 37(4):494-500, 1997. [13] Plyavin' YA and Blum EY. *Magnetohydrodynamics*, 16(4):349-59, 1983. [14] Yamauchi H et al. *J Neurol Neurosurg Psychiatr*, 61(1):18-25, 1996. [15] Yamada N et al. *Radiology*, 198(1):171-8, 1996. [16] Kressler B et al. *ISMRM*, p1514, 2008.
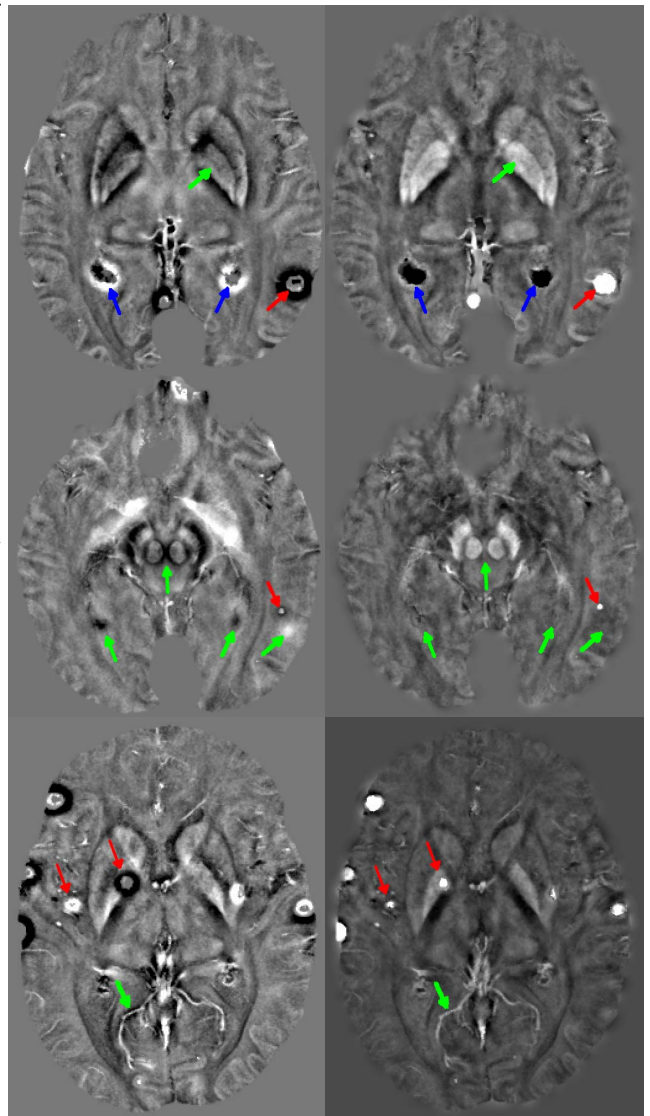
FIG. 1: Representative transverse slices of pre-processed phase data (left) and corresponding susceptibility maps (right) of patient B (top, middle) and patient A (bottom). Red and blue arrows mark exemplary hemorrhages and calcifications, respectively.